JPE 17-5-18

https://doi.org/10.6113/JPE.2017.17.5.1308
ISSN(Print): 1598-2092 / ISSN(Online): 2093-4718

Submodule Level Distributed Maximum Power Point Tracking PV Optimizer with an Integrated Architecture

Feng Wang†, Tianhua Zhu*, Fang Zhuo*, Hao Yi*, and Shuhuai Shi*

†,*State Key Laboratory of Electrical Insulation and Power Equipment, Xi'an Jiaotong University, Xi'an, China

Abstract

The distributed maximum power point tracking (DMPPT) concept is widely adopted in photovoltaic systems to avoid mismatch loss. However, the high cost and complexity of DMPPT hinder its further promotion in practice. Based on the concept of DMPPT, this paper presents an integrated submodule level half-bridge stack structure along with an optimal current point tracking (OCPT) control algorithm. In this full power processing integrated solution, the number of power switches and passive components is greatly reduced. On the other hand, only one current sensor and its related AD unit are needed to perform the ideal maximum power generation for all of the PV submodules in any irradiance case. The proposal can totally eliminate different small-scaled mismatch effects in real-word condition and the true maximum power point of each PV submodule can be achieved. As a result, the ideal maximum power output of the whole PV system can be achieved. Compared with current solutions, the proposal further develops the integration level of submodule DMPPT solutions with a lower cost and a smaller size. Moreover, the individual MPPT tracking for all of the submodules are guaranteed.

Key words: Ideal maximum power generation, Mismatch, PV, Submodule

I. INTRODUCTION

Photovoltaic (PV) systems have been widely built all over the world to directly utilize solar energy. Since ideal irradiance is practically impossible in the real-world, PV panels often suffer from different shading cases in daily operation. Moreover, non-uniform aging and the accidental damage of PV panels frequently occur and have a negative impact on the performance of PV systems, especially in the middle and late periods of their service life. The aforementioned cases can be collectively called mismatches. Due to the difficult predictions of shading cases and the high cost of replacing aged (or damaged) PV units with new ones, the mismatches in PV systems significantly deteriorate the effectiveness of the energy harvest, particularly in centralized and string level maximum power point tracking (MPPT) based PV systems. Moreover, mismatches cases also lead to multiple maximum power points (MPP) on the power-voltage curve of original PV arrays or PV strings which leads to a failure of most MPPT algorithms and power oscillations [1]-[3].

Therefore, it is appealing to improve the energy efficiency of PV systems in mismatch cases. Distributed maximum power point tracking (DMPPT) PV systems have drawn increased attention because it decouples the PV units from the adjacent ones through a dedicated MPPT converter. The module level MPPT converter, commonly referred to as a "PV optimizer" or "module integrated converter (MIC)," has been widely explored and is essentially concerned with current PV systems. Since small-scale mismatch cases happens more frequently, such as in portable solar power systems, the performance of current commercial PV optimizer-based solar systems is still less than satisfactory in such cases. Submodule level DMPPT solutions have developed rapidly in recent years. Submodule level MPPT can be regarded as a further step to address small-scale mismatch issues with better power recovery capability. Submodule DMPPT converters are designed to fit the junction box of commercial PV panels and perform MPPT at the submodule level to eradicate small scale mismatch power losses.

Manuscript received Feb. 3, 2017; accepted May 25, 2017
Recommended for publication by Associate Editor M. Vilathgamuwa.
†Corresponding Author: fengwangee@xjtu.edu.cn
Tel: +86-29-82668666, Xi'an Jiaotong University
*State Key Laboratory of Electrical Insulation and Power Equipment, Xi'an Jiaotong University, China

Although mismatch losses can be recovered through submodule DMPPT with independent MPPT control, the implementation costs of the system multiply due to the increasing number of components. A set of power switches, passive devices (inductors and capacitors), MPPT control ICs, current sensors, voltage sensors and corresponding AD/DA converters are needed for every PV submodule. Since the PV market is cost-sensitive, increasing the number of components results in increases in high, weight, size and cost, as well as a lower efficiency and index of mean time before failure (MTBF). The above drawbacks prevent the submodule DMPPT concept from spreading and becoming popular. The maximum power point (MPP) voltage (Vmpp) is not a strong function of irradiance, unlike the MPP current Impp. As a result, many methods have been proposed to simplify the submodule level DMPPT solutions. In [4], a unified input voltage control strategy is proposed which can recover nearly all of the power loss caused by small scaled mismatch cases. In [5], a close-to-optimal distributed control approach is presented that allows autonomous submodule control without the need for a central controller or any communication among the PV submodules. Although the above methods are proposed with reduced cost and fewer components, both of them are still quasi-MPPT solutions. In fact, with "virtual parallel" operation, the operating voltages of the PV submodules are regulated to be equal while the physical series connection of the DC-DC converters is maintained to achieve enough output voltage. The authors of [6], [7] utilized a Gallium-Nitride device in a submodule Buck converter to achieve a high conversion efficiency and a reduced size. Nonetheless, higher cost is still a bottleneck for large-scale enterprise applications. In [8], [9], time-sharing MPPT control solutions are proposed and the true MPP of each PV submodule can be achieved. However, the number of components in the circuit is not satisfying from a cost perspective. In [3], [10], differential power processing structure based submodule DMPPT solutions are proposed. These structures only processes the partial power generated from PV units with an inherently high efficiency when compared with other full power processing methods. Nonetheless, the complexity of this MPPT algorithm makes it difficult to promote and the neighboring submodules cannot be easily decoupled from each other. It has been shown in [11], [12] that tracking the output current can realize MPPT functionality with a greatly reduced number of sensors and a further simplified controller and inductor.

In this paper, an integrated half-bridge stack structure with a common LC filter is used in a submodule distributed power generation system. In this full power processing structure, an optimal current point tracking (OCPT) control strategy is applied. It only requires one current sensor, one AD unit and one digital controller for performing submodule level maximum power tracking control. This proposal can totally eliminate the small-scaled mismatch effects in real-word

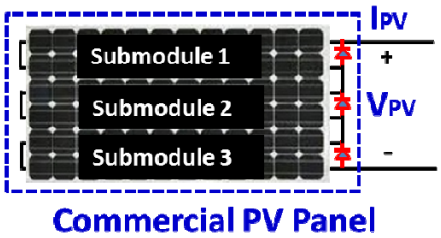

Fig. 1. Structure of a commercial PV panel.

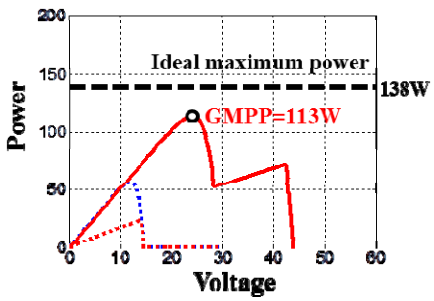

Fig. 2. Output P-V curve of a shaded PV panel.

conditions, and the ideal maximum power point of each PV submodule can be achieved precisely even under irradiance changes. Compared with current solutions, the proposed method further develops the integration level of submodule DMPPT solutions with fewer components, lower cost, smaller size and a higher MTBF index. Simulation and experimental results show that the ideal MPPs of the submodules can be exactly reached separately.

II. Analysis of the Proposed Integrated Solution

A. Shading Case Study

For centralized or string level MPPT PV systems, the consequences of a mismatch are degradations in the total power harvest and multiple maxima power points issues on the power-voltage curve. The global maximum power point (GMPP) of a shaded PV system can be reached through some advanced algorithms. However, such a power is still lower than the ideal maximum power which is the sum of the available maximum powers for each of the PV units, since the shaded part of the PV system limits the output current of the non-shaded part [13], [14]. Fig.1 shows a standard PV panel consisting of PV cells connected in series. They are divided into three submodules by anti-parallel bypass diodes which help reduce the appearance of hot spots and to mitigate the destructive effects in the PV submodules.

Fig. 2 shows the mismatch case where submodule 3 is shaded. The output P-V curves of submodules 1 and 2 are shown as blue dotted lines. The output P-V curve of submodule 3 is shown as a red dotted line. The output P-V

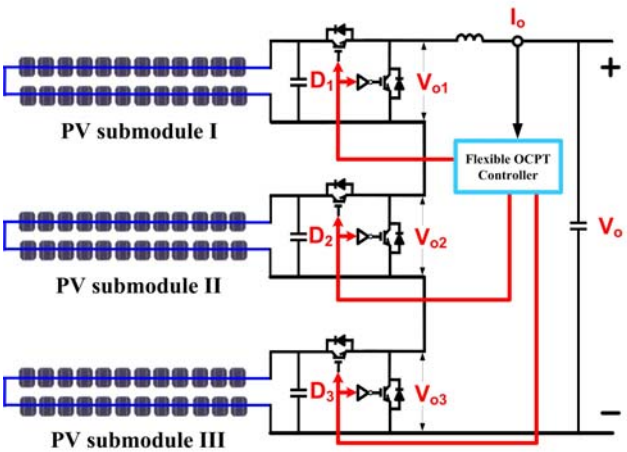

Fig. 3. Structure of a power circuit.

curve of this partially shaded PV panel is depicted as a red solid curve. The black dashed line indicates the ideal maximum power of the PV panel (138W), which is about 18% higher than the value of the GMPP (113W) in this case.

Functionally, current commercial PV optimizers can only achieve the GMPP point of the red curve shown in Fig.2. The mismatch power loss cannot be totally recovered. The topologies of current solutions can be classified into three categories according to their voltage gain: Buck type, Boost type and Buck-Boost type. The pros and cons of these solutions have already been analyzed in detail in previous studies [4], [15], [16].

B. Power Circuit

In this paper, a synchronized Buck converter stack with a common LC filter is adopted as the topology of a submodule maximum power generation system due to its simpler structure, reduced number of components and easier achievements of MPPT in a series connection.

As shown in Fig.3, the input side of each buck converter is connected in parallel with a PV submodule. From the output sides, these inductor-free buck converters are connected in series to achieve a higher output voltage with a common LC filter. Each half bridge is separately controlled by a pair of complementary duty cycle signals (eg. D_1 and (1-D_1)). In this structure, lower power rating devices and a higher voltage gain can be adopted for submodule PV applications. This structure can be directly connected to the DC bus or DC link of a commercial micro-inverter to perform grid-tied power generation. In this structure, the single capacitor is smaller than the total combined set of capacitors if an interleaving carrier is adopted, which is normally used with every buck DC-DC converter. The use of a single inductor also reduces cost and weight while increasing the efficiency in extracting the maximum power from PV submodules.

For this architecture, a static working principle analysis is conducted below. Under steady state conditions, the output voltage of each Buck converter and its corresponding PV submodule voltage satisfy equation (1).

$$\frac{V_{o1}}{V_{pv1}} = D_1, \frac{V_{o2}}{V_{pv2}} = D_2, \frac{V_{o3}}{V_{pv3}} = D_3, . \tag{1}$$

Similarly, the total output current and each of the photovoltaic currents satisfy equation (2).

$$I_o = \frac{I_{pv1}}{D_1} = \frac{I_{pv2}}{D_2} = \frac{I_{pv3}}{D_3} \tag{2}$$

Since the average value of the voltage across the single inductor L can be considered 0 over a switching period, V_o is expressed as:

$$V_o = \sum_{i=1}^{3} V_{oi} = \sum_{i=1}^{3} V_{pvi} \cdot D_i = \sum_{i=1}^{3} V_{pvi} \cdot \frac{I_{pvi}}{I_o} \tag{3}$$

Obviously:

$$V_o \cdot I_o = \sum_{i=1}^{3} V_{pvi} \cdot I_{pvi} \tag{4}$$

From the above equations, it can be noted that regardless of the mismatch conditions of PV submodules, the output power for all of the submodules can be obtained at the general output side. Thus, all of the submodules can operate at their individual MPPs and the ideal maximum output power can be extracted from the PV units.

C. Simplified OCPT Control Strategy

The DC voltage (V_o) is mostly controlled by micro-inverter which can be regarded as a controllable current sink. Since the perturbation interval of the 2nd maximum power seeking process is much longer than that in the submodule level converters, V_o can be considered temporarily fixed during the perturbation of the Buck converters. With a given V_o, maximizing the string current (I_o) is equivalent to maximizing the total output power with a fixed V_o. Therefore, the half bridges, as shown in Fig.3, iterate frequently to maximize the total output current I_o for a given V_o, which is exactly the fundamental principle of the proposed OCPT strategy.

In the proposed system, time-sharing OCPT control is adopted on the output side of the module so that only one controller is sufficient. A flow diagram of this control strategy is presented in Fig.4 (b). The parameter clock is progressively increased and its value decides which submodule is to be tracked. For example, if the value of the clock is between 0 and T, this means that the controller is doing OCPT for submodule 1. Similarly, when the clock is between T and 2T, submodule 2 is under OCPT. When clock exceeds 3T, it is reset to 0 and the above process is repeated.

As aforementioned, the output voltage V_o in Fig.3 can be considered to be temporarily constant. According to equations (3) and (4), the variation of I_o can just represent the variation of the total output power P_o. In addition, in [17], the single output parameter MPPT control is shown to be possible for nearly all practical load types. Consequently, a

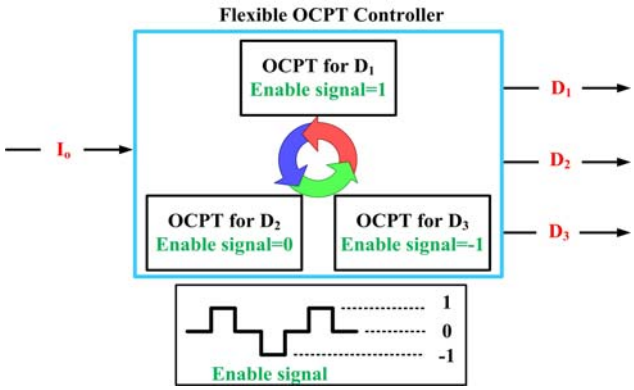

(a) Schematic of an OCPT block.

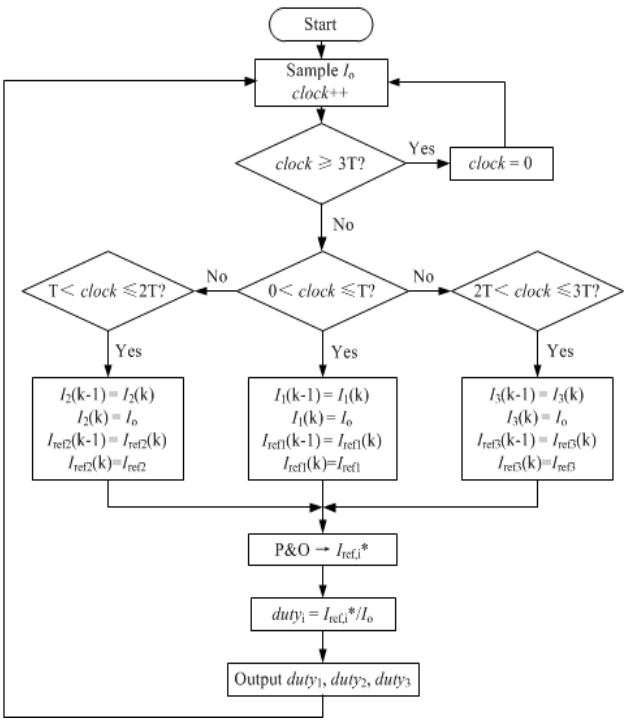

(b) Flow chart of time-sharing OCPT control.

Fig. 4. Diagram of a control block.

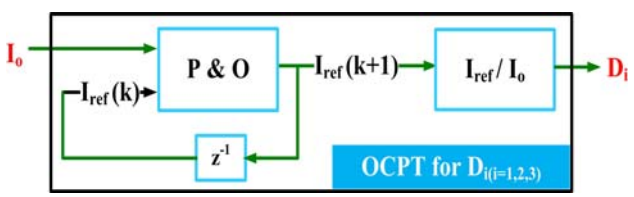

Fig. 5. Directly duty cycle controller.

single current sensor for the output current I_o is sufficient to achieve maximum power generation control.

Fig. 5 shows the working principle of the direct duty cycle controller. The single current sensor based OCPT controller seeks the MPP on the PV submodules in turn. This means that at any time, the variation of the total output power P_o is equal to the power variation of the submodule being tracked. A Perturb and Observe (P&O) algorithm is adopted to impose a perturbation on the photovoltaic current of the submodules instead of the typical photovoltaic voltage. Generally, a P-I curve has a similar shape to a P-V curve. Hence, according to the sign of $\Delta I_o(k)\cdot\Delta I_{ref}(k)$, the current reference of the next period $I_{ref}(k+1)$ can be derived. Then the objective duty ratio can be calculated as: $D(k+1)= I_{ref}(k+1)/I_o$ and the PWM signal of this duty cycle is generated by the OCPT controller to drive the relative switch and bring the photovoltaic current to the expected reference. The direct duty cycle control no longer needs to detect the real-time voltage for each of the PV submodules. As a result, three voltage sensors are eliminated.

III. Comparison with Current Solutions

Several related papers are compared to justify the improvement of the proposed solution. The comparison is given from following aspects: number of power components required in the power circuit, number of control related components in the control part and other characteristics of the integrated PV module. Before the comparison, several features need some explanation. The ideal maximum power indicates the sum of the available maximum powers for each of the PV units as shown in Fig.2. The output power ratio indicates the normalized ratio of the actual output power to the ideal maximum power. The voltage gain shows the ratio of the output voltage of the integrated PV module to the voltage of the PV submodule. The optimal power region means the feasible voltage (or current) region of the DMPPT PV system which makes all of the PV units work on their individual MPPs in given irradiance cases [15].

The five latest related solutions are selected to execute the comparative analysis. Together with the proposed solution, six methods are studied and compared from different perspectives. The counterparts are referred to as follows:

A. Control Strategy I: [6], [7];

Control strategy I introduces an independent MPPT control for each of the PV submodules inside a standard PV panel and it regulates the duty cycle of the power stage separately in order to decouple a PV submodule from the other submodules in a PV panel. Gallium-Nitride devices are used to achieve high conversion efficiency and a reduced size. Nonetheless, a higher cost is still the bottleneck for large-scale enterprise applications.

B. Control Strategy II: [4], [17], [18];

A unified output voltage strategy with a single MPPT controller is referred to as Control strategy II. In this structure:

1) A single MPPT unit is used to sense the total output power of a converter system with only one pair of voltage and current sensors;

TABLE I
COMPARATIVE ANALYSIS

		Technique I	Technique II	Technique III	Technique IV	Technique V	Our paper
Components in Power circuit	Inductors	***n***	***n***	***n***	***n***	1	1
	Switches	2n	2n	2n	2n	***2n+2***	2n
	Capacitors	***2n***	***2n***	***2n***	n+1	n+1	n+1
Components in control circuit	Control Units	***n***	1	1	1	1	1
	Sensor and related AD converter	***2n***	n+2	n+1	1	1	1
Other characteristics	Ideal maximum power	Y	***N***	Y	Y	***N***	Y
	Output power ratio	1	1	1	1	***1/N***	1
	Voltage gain	high	high	high	***low***	***low***	high
	Optimal power region	Y	***N***	Y	Y	***N***	Y

2) Three Buck MPPT converters share a common V_{ref} coming from the single MPPT unit;

3) Each Buck MPPT converter has an independent control loop. This control method only achieves a quasi-MPPT state.

"Virtual parallel" operation is introduced so that the operating voltages of the PV submodules are regulated to be equal under different mismatch cases, while the physical series connection of the dc/dc converters is maintained.

From (21), it is clear that the characteristics of the PI type back-EMF estimator are the same as those of a first-order low-pass filter.

C. Control Strategy III: [8];

Based on Control strategy II, Control strategy III is applied to multi-panel level simplification. The unified output control is applied to each of the PV panels and the multiple unified controllers of four PV panels are optimized through time sharing MPPT control. In this structure, the number of MPPT ICs is decreased by the time-sharing control strategy of the four buck converters and the related PV panels. The output voltage of the buck converters and total output current are sampled as inputs for the MPPT control unit. Under the control of a periodic enable signal, the MPPT unit operates a P&O algorithm for the corresponding buck converter and outputs a PWM signal of a certain duty ratio for its power MOSFET.

D. Control Strategy IV: [11];

In control strategy IV, a distributed MPPT realization with a better simplification design is given. The single sensor maximum power tracking strategy was proposed and achieved fast tracking performance due to its two-mode operation. This architecture requires only one sensor and the MPPT function is able to be performed for each of the submodule PV units through the switch and the common MPPT converter. However, the output for each of the MPPT converters is connected in parallel which greatly reduces the voltage gain of the system. Moreover, three inductors are still needed. Hence, there is an opportunity to improve this strategy.

E. Control Strategy V: [12];

Based on the single sensor technique in control strategy IV, this strategy further optimizes the power circuit and reduces the system complexity and cost. A multi-channel PV system with a single sensor MPPT controller is proposed to track the MPP for each of the PV units. The number of components (capacitors, current sensors, voltage sensors, MPPT controllers, etc.) is decreased in this paper. However, due to the limitation of the power circuit, only one PV submodule can output its power at any time during operation. In addition, two additional switches are needed when compared to the other solutions. The requirement for too many converters and a high cost is a big issue for further application.

F. The Proposed Strategy;

In this paper, a three buck stack structure with a common LC filter is applied to the submodule mismatch issue. An OCPT control algorithm is applied to make full utilization of one current sensor, one AD unit and one digital controller. The proposal can completely eliminate different small-scaled mismatch effects under real-word conditions and the true maximum power point of each PV submodule can be achieved precisely even under a rapid irradiance change. For example, compared with control strategy V, the complexity of the power circuit is further optimized in the proposed method. In addition, the number of power switches is only $2N$, which is less than that in control strategy V ($2N$+2). The voltage gain of the circuit proposed in this paper is three times as high as that in control strategy V, which means another high voltage gain cascading converter is still needed if control strategy V is used in grid-tied power generation. In control strategy V, the circuit only outputs the maximum power of the connected PV unit while the other disconnected units are totally lost without any power output. The operating state for each of the PV units depends on the enable switch (S_{u1}, S_{u2},…,S_{uN}). In this paper, all of the PV units output their individual maximum power at any time regardless of the mismatch case.

Based on the above analysis from different perspectives,

TABLE II
PARAMETERS FOR THE SYSTEM VERIFICATIONS

Parameters		Value
PV Submodules	V_{mpp1}, I_{mpp1}, P_{mpp1} (STC)	10V, 2A, 20W
	V_{mpp2}, I_{mpp2}, P_{mpp2} (STC)	12.5V, 2.5A, 31.25W
	V_{mpp3}, I_{mpp3}, P_{mpp3} (STC)	15V, 3A, 45W
Control Unit	f_s	20kHz
	T_{mppt}	0.05s
	T	20ms

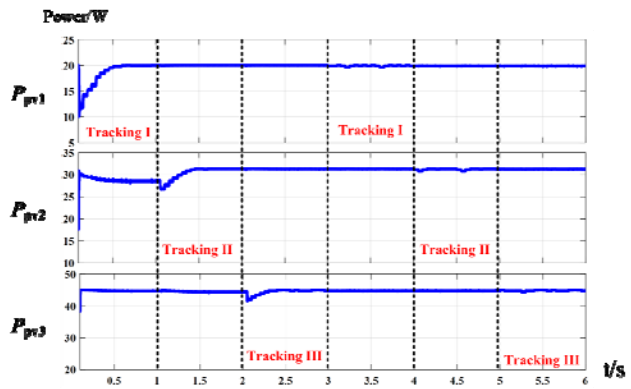

Fig. 6. Voltage waveforms of three submodules.

the pros and cons have been summarized in Table I. When compared with other solutions, the solution in this paper proposes an optimized submodule level PV system. It can be integrated into the junction box of commercial PV modules. The proposed system can guarantee ideal maximum power generation for each of the PV units regardless of mismatch cases. This is accomplished with the lowest number of components in both the power circuit and the control circuit when compared with other full power processing solutions.

IV. SIMULATION AND TEST RESULTS

Simulation and hardware test results are provided to verify the proposed structure and strategy. Several of the related parameters are given in TABLE.II.

A. Simulation Results

Simulation performance is shown in Fig. 6, which presents the voltage waveforms of the three submodules. During the first second, submodule 1 is being tracked and it arrives at its MPP voltage. Then in the next second, the MPPT controller tracks submodule 2 and finally makes it operate at its MPP voltage and outputs 31.25W of power. In the next period (2s, 3s), submodule 3 is being perturbed and reaches its MPP. At this moment, all of the submodules operate at their respective MPPs and the process repeats. Since all of the submodules have reached their MPPs, there are only slight oscillations around the MPP voltages in the second round of tracking.

The above simulation results effectively verify that with the OCPT control strategy, the proposed integrated structure can make all of its submodules operate at their individual MPPs regardless of mismatch cases.

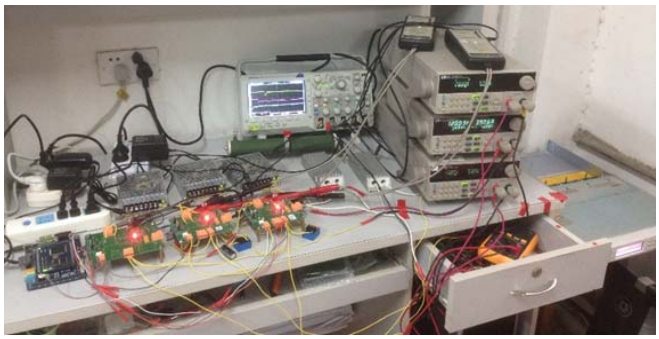
Fig. 7. Testbed.

TABLE III
PARAMETERS OF THE OCPT BASED PV MODULE

Parameters		Value
Test cases	V_{mpp1}, V_{mpp2}, V_{mpp3} (**Case 1**)	10V, 10V,10V
	V_{mpp1}, V_{mpp2}, V_{mpp3} (**Case 2**)	10V, 12.5V,15V
Control Unit	f_s	50kHz
	T_{mppt}	1s
	T	25s

B. Test Results

To further verify the effectiveness of the proposed scheme, an experimental validation is carried on and the testbed is shown in Fig.7. A DC voltage source and a series connected power resistor are used to replicate the electrical behavior of a sunlight illuminated PV module in an indoor environment. The output of the proposed structure is connected to an electronic load. Two different cases are tested, as listed in Table III.

In case 1, all of the submodules are under the same irradiance without any mismatch. Fig.8 shows the voltage waveforms of three submodules. (Blue: 1; Purple: 2; Green: 3) In the first 25 seconds, submodule 1 is being tracked, while submodules 2 and 3 are waiting for MPPT. It takes about 8s to reach a Vmpp1 of 10V and then Vpv1 keeps oscillating around 10V. At 25s, the OCPT controller turns to track the MPP for submodule 2 and Vpv2 finally arrives at 10V. During the interval of (50s, 75s), the MPPT of submodule 3 is enabled and Vmpp3 is approached. At 75s, all of the submodules operate at their respective MPPs and there are only slight oscillations around the MPP voltages in the second round of tracking, as shown in Fig. 8.

In case 2, three submodules are under different irradiances.

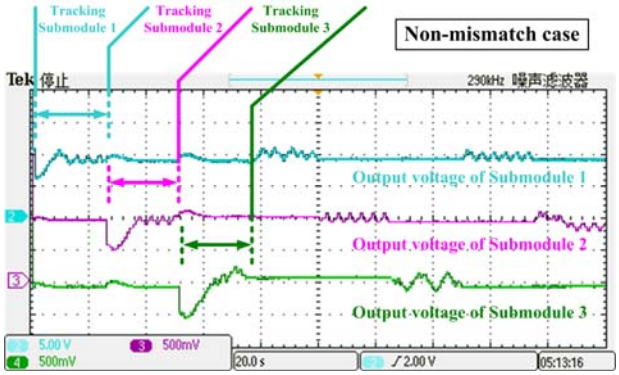

Fig. 8. Test results of Case 1.

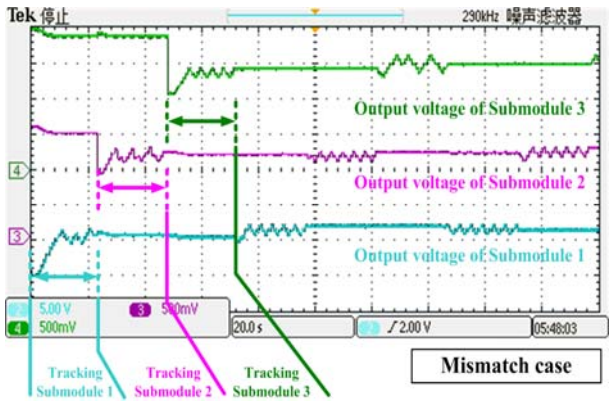

Fig. 9. Test results of Case 2.

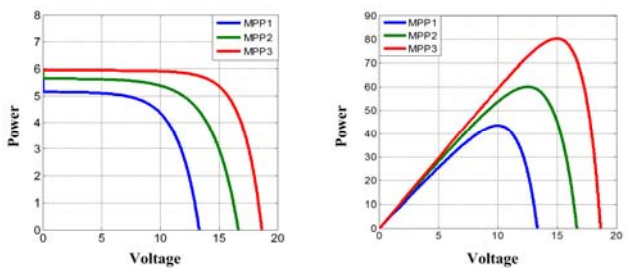

Fig. 10. Testbed.

Fig.9 shows voltage waveforms of the three submodules of this case (Blue: 1; Purple: 2; Green: 3). The operating process is similar to case 1, while the three submodules reach different MPPs. Submodule 1 is tracked first, while submodules 2 and 3 are waiting for MPPT. Vpv1 reaches a Vmpp1 of 10V and keeps oscillating around 10V. During the interval of (25s, 50s), the MPPT of submodule 2 is activated and Vmpp2 is approached. At 50s, the OCPT controller turns on to perturb the voltage of submodule 3 and Vpv3 finally arrives at 15V. After submodule 3 has achieved its MPPT, all of the submodules output their respective maximum powers. Unless irradiance changes, there are only slight oscillations around the MPP voltages in the next round of tracking.

Since the output voltages of the three submodules are not common ground, one ordinary probe (channel 2) is used to measure the output voltage of submodule I, and two differential probes (channel 3 and 4) are used to measure the output voltages of submodules 2 and 3, respectively. The differential probe zooms out the measured voltage and the ratio is 10:1. Therefore, the scales of channel 3 and 4 are 500mV. In the experiment case 1, the MPP voltages of the three submodules are all 10V, and the P-V and I-V curves are shown as blue curves in Fig.10. It can be seen in Fig.8 that all of the submodules reach 10V. Similarly, in case 2, the MPP voltages of the three submodules are supposed to be 10V, 12.5V and 15V. It can be seen in Fig.9 that the three submodules indeed reach 10V, 12.5V and 15V. Therefore, the MPP tracking capability is sufficiently verified.

It can be seen that the experimental results validate the effectiveness and viability of the proposed scheme. Using the OCPT control strategy, the submodule level Buck stack structure can precisely track the individual MPPs for all of the submodules regardless of mismatch cases.

V. CONCLUSIONS

Simplification and optimization have been the goals of the development of DMPPT PV systems especially in submodule level applications. However, there is always a tradeoff between the mismatch power loss and an increase in the number of components. This paper proposed a submodule level maximum power generation solution against small scale shading in real-world cases. The proposed integrated submodule level PV structure along with an OCPT control strategy can eliminate mismatch power loss. They also enjoy the smallest number of components when compared with the current solutions in the literature. Meanwhile, the true MPP for each of the PV submodules can always be guaranteed even under rapid irradiance changes. The proposed low-cost submodule DMPPT solution and control algorithm provide very promising power savings when compared to the conventional MPPT approach. The enormous potential of the proposed system with its limited control unit and components can be developed to achieve more integrated, modularized, intellectual PV systems in the future.

ACKNOWLEDGMENT

This work was supported in part by Natural Science Foundation of China (No: 51407133), in part by Natural Science Foundation of Shaanxi (No: 2017JQ5049), in part by the China Postdoctoral Science Foundation 2016T90919.

REFERENCES

[1] S. Qin, C. B. Barth, and R. C. N. Pilawa-Podgurski, "Enhancing microinverter energy capture with submodule differential power processing," *IEEE Trans. Power Electron.*, Vol. 31, No. 5, pp. 3575-3585, May 2016.

[2] K. A. Kim, P. S. Shenoy, and P. T. Krein, "Converter rating analysis for photovoltaic differential power processing systems," *IEEE Trans. Power Electron.*, Vol. 30, No. 4, pp. 1987-1997, Apr. 2015.
[3] Y. T. Jeon, H. Lee, K. A. Kim, and J. H. Park, "Least power point tracking method for photovoltaic differential power processing systems," *IEEE Trans. Power Electron.*, Vol. 32, No. 3, pp. 1941-1951, Mar. 2017.
[4] F. Wang, X. Wu, F. C. Lee, Z. Wang, P. Kong, and F. Zhuo, "Analysis of unified output MPPT control in subpanel PV converter system," *IEEE Trans. Power Electron.*, Vol. 29, No. 3, pp. 1275-1284, Mar. 2014.
[5] C. Olalla, D. Clement, M. Rodriguez, and D. Maksimovic, "Architectures and control of submodule integrated DC-DC converters for photovoltaic applications," *IEEE Trans. Power Electron.*, Vol. 28, No. 6, pp. 2980-2997, Jun. 2013.
[6] O. Khan, W. Xiao, and H. H. Zeineldin, "Gallium-nitride-based submodule integrated converters for high-efficiency distributed maximum power point tracking PV applications," *IEEE Trans. Ind. Electron.*, Vol. 63, No. 2, pp. 966-975, Feb. 2016.
[7] R. C. N. Pilawa-Podgurski and D. J. Perreault, "Submodule integrated distributed maximum power point tracking for solar photovoltaic applications," *IEEE Trans. Power Electron.*, Vol. 28, No. 6, pp. 2957-2967, Jun. 2013.
[8] Z. Cao, Q. Li, and F. C. Lee, "Multi-phase smart converter for PV system," in *IEEE Applied Power Electronics Conference and Exposition (APEC),* pp. 1736-1742, Mar. 2015.
[9] F. Wang, T. Zhu, F. Zhuo, H. Yi, S. Shi, and X. Zhang, "Analysis and optimization of flexible MCPT strategy in submodule PV application," *IEEE Trans. Sustain. Energy,* Vol. 8, No. 1, pp. 249-257, Jan. 2017.
[10] S. Qin, S. T. Cady, A. D. Dominguez-Garcia, and R. C. N. Pilawa-Podgurski, "A distributed approach to maximum power point tracking for photovoltaic submodule differential power processing," *IEEE Trans. Power Electron.*, Vol. 30, No. 4, pp. 2024-2040, Apr. 2015.
[11] J. A. A. Qahouq and Y. Jiang, "Distributed photovoltaic solar system architecture with single-power inductor single-power converter and single-sensor single maximum power point tracking controller," *IET Power Electronics*, Vol. 7, No. 10, pp. 2600-2609, Oct. 2014.
[12] Y. Jiang and J. A. A. Qahouq, "Single-sensor multi-channel maximum power point tracking controller for photovoltaic solar systems," *IET Power Electronics*, Vol. 5, No. 8, pp. 1581-1592, Sep. 2012.
[13] S. Lyden and M. E. Haque, "A simulated annealing global maximum power point tracking approach for PV modules under partial shading conditions," *IEEE Trans. Power Electron.*, Vol. 31, No. 6, pp. 4171-4181, Jun. 2016.
[14] M. Seyedmahmoudian, R. Rahmani, S. Mekhilef, A. M. T. Oo, A. Stojcevski, T. K. Soon, and A. S. Ghandhari, "Simulation and hardware implementation of new maximum power point tracking technique for partially shaded PV system using hybrid DEPSO method," *IEEE Trans. Sustain. Energy,* Vol. 6, No. 3, pp. 850-862, Jul. 2015.
[15] F. Wang, F. Zhuo, F. C. Lee, T. Zhu, and H. Yi, "Analysis of existence-judging criteria for optimal power regions in DMPPT PV systems," *IEEE Trans. Energy Convers.,* Vol. 31, No. 4, pp. 1433-1441, Dec. 2016.
[16] W. Xiao, N. Ozog, and W. G. Dunford, "Topology Study of photovoltaic interface for maximum power point tracking," *IEEE Trans. Ind. Electron.*, Vol. 54, No. 3, pp. 1696-1704, Jun. 2007.
[17] D. Shmilovitz, "On the control of photovoltaic maximum power point tracker via output parameters," *IEE Proceedings – Electric Power Applications*, Vol. 152, No. 2, pp. 239-248, Mar. 2005.
[18] S. Poshtkouhi, J. Varley, R. Popuri, and O. Trescases, "Analysis of distributed peak power tracking in photovoltaic systems," in *International Power Electronics Conference (IPEC),* pp. 942-947, Jun. 2010.
[19] L. Xiong, F. Zhuo, F. Wang, X. Liu, Y. Chen, M. Zhu, and H. Yi, "Static synchronous generator model: a new perspective to investigate dynamic characteristics and stability issues of grid-tied PWM inverter," *IEEE Trans. Power Electron.*, Vol. 31, No. 9, pp. 6264-6280, Sep. 2016.

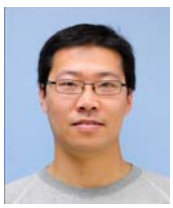

Feng Wang (S'08, M'13) received his B.S., M.S. and Ph.D. degrees in Electrical Engineering from Xi'an Jiaotong University (XJTU), Xi'an, China, in 2005, 2009 and 2013, respectively. From November 2010 to November 2012, he was an exchange Ph.D. student in the Center for Power Electronics Systems (CPES) at the Virginia Polytechnic Institute and State University, Blacksburg, VA, USA. In November 2013, he joined XJTU as a Postdoctoral Fellow. His current research interests include DC/DC conversions and the digital control of switched converters, especially in renewable energy generation field. Dr. Wang is with the State Key Laboratory of Electrical Insulation and Power Equipment, School of Electrical Engineering, XJTU.

Tianhua Zhu (S'16) received her B.S. degree in Electrical Engineering from Xi'an Jiaotong University (XJTU), Xi'an, China, in 2014, where she is presently working towards her M.S. degree in the Power Electronics and Renewable Energy Center (PEREC). Her current research interests include maximum power point tracking techniques, distributed maximum power point tracking and differential power processing. She is presently with the State Key Laboratory of Electrical Insulation and Power Equipment, School of Electrical Engineering, XJTU.

Fang Zhuo (M'00) was born in Shanghai, China, in 1962. He received his B.S. degree in Automatic Control, and his M.S. and Ph.D. degrees in Automation and Electrical Engineering from Xi'an Jiaotong University (XJTU), Xi'an, China, in 1984, 1989 and 2001, respectively. He became an Associate Professor at XJTU in 1996, and a Full Professor of Power Electronics and Drives in 2004. Then he worked as a supervisor of Ph.D. students. His current research interests include power electronics, power quality, active power filters, reactive power compensation, inverters for distributed power generation, etc. He is the key finisher of four projects sponsored by the National Natural Science Foundation of China, and more than 40 projects in cooperation with companies in the industry. He received four provincial and ministerial level science and technology advancement awards. In addition, four patents are pending or owned by him. He is a member of the China Electro Technical Society, the Automation Society, and the Power Supply Society. He is also the Power Quality Professional Chairman of the Power Supply Society in China.

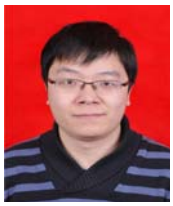

Hao Yi (S'10–M'14) received his M.S. and Ph.D. degrees in Electrical Engineering from Xi'an Jiaotong University (XJTU), Xi'an, China, in 2010 and 2013, respectively. Since 2013, he has been a Member of the School of Electrical Engineering at XJTU. His current research interests include the modeling and control of high-power converters, the control and power management of microgrids, and power quality improvement.

Shuhuai Shi(S'15) received his B.S. degree in Electrical Engineering from the Henan Polytechnic University, Jiaozuo, China, in 2012. He is presently working towards his Ph.D. degree in the State Key Laboratory of Electrical Insulation and Power Equipment, School of Electrical Engineering, Xi'an Jiaotong University (XJTU), Xi'an, China. His research interests include the topologies, control and modulation of high voltage and high power DC/DC converters, and the modeling and control of modular multilevel converters.